Uranium deposits in the Espanola Basin, Santa Fe County, New Mexico

Virginia T. McLemore, David Vaniman, Dennis McQuillan, and Patrick Longmire, 2011, pp. 399-408

in:

Geology of the Tusas Mountains and Ojo Caliente, Author Koning, Daniel J.; Karlstrom, Karl E.; Kelley, Shari A.; Lueth, Virgil W.; Aby, Scott B., New Mexico Geological Society 62nd Annual Fall Field Conference Guidebook, 418 p.

This page is intentionally left blank to maintain order of facing pages.

URANIUM DEPOSITS IN THE ESPAÑOLA BASIN, SANTA FE COUNTY, NEW MEXICO

VIRGINIA T. MCLEMORE[1], DAVID VANIMAN[2], DENNIS MCQUILLAN[3], AND PATRICK LONGMIRE[2]
[1]New Mexico Bureau of Geology & Mineral Resources, New Mexico Institute of Mining & Technology, Socorro, NM 87801; ginger@gis.nmt.edu
[2]EES-6, MS D469, Los Alamos National Laboratory, Los Alamos, New Mexico 87545
[3]New Mexico Environment Department, 525 Camino de los Marquez, Suite 1, Santa Fe, New Mexico 87505

ABSTRACT—Uranium mineralization in the Española Basin is not of sufficient quantity and quality to justify mining at the present time. However, many private water wells in the region produce water with concentrations of uranium (up to 1,820 µg/L (ppb)) that exceed the safe drinking water standard of 30 µg/L. Therefore, it is important to understand the source of the uranium in the groundwater and the processes involved. Potential sources for uranium in the groundwater include 1) uranium occurrences in the Tesuque Formation (San Jose mining district), 2) rhyolitic volcanic ash beds and sandstones with volcanic detritus found interbedded within the Tesuque Formation, 3) veins, replacements, and pegmatites in Proterozoic rocks (San Jose and Nambe mining districts), and 4) Proterozoic granitic rocks in the Sangre de Cristo Mountains.

The sandstone uranium occurrences in the Tesuque Formation represent natural precipitation and concentration from uraniferous groundwaters, likely derived from 1) rhyolitic volcanic ash beds within the Tesuque Formation, 2) the alteration of granitic and/or volcanic detritus within the sedimentary host rocks, and 3) Proterozoic rocks in the Sangre de Cristo Mountains to the east. One property, the San Jose No. 13 (NMSF0033), produced 12 lbs (5 kg) of U_3O_8 at a grade of 0.05% U_3O_8 in 1957. Uranium in modern groundwaters likely was derived from the same sources, as well as from leaching and oxidation of older uranium occurrences in the Tesuque Formation. Uranium then precipitated from the waters to form the geochemical anomalies found in the prospects.

INTRODUCTION

Many residents in the Española Basin in Santa Fe County, New Mexico, have high concentrations of uranium and radon in their drinking water (McQuillan et al., 2005; Johnson et al., 2008) and high concentrations of uranium are found in both NURE (National Uranium Resource Evaluation) water and stream-sediment samples (Figs. 1, 2, 3; McLemore, 2010a, b). Uranium has been detected in approximately 50% of the water supply wells in this area at concentrations exceeding the drinking water standard of 30 µg/L (ppb). At least 27 wells serving 19 public water systems, and 209 private domestic wells, produce water with excessive uranium. Concentrations range from less than 1 µg/L to a maximum of 1,820 µg/L (McQuillan et al., 2005). The isotopic signature of this water is consistent with a natural source of uranium (McQuillan et al., 2005; Johnson et al., 2008). In addition, high concentrations of uranium are found in water used for irrigation in some areas, and since some plants can uptake uranium, uranium could become elevated in these plants (Hakonson-Hayes et al., 2002). High uranium in drinking water can cause kidney toxicity. Furthermore, high levels of indoor radon are widespread in this region (McQuillan et al., 2005). EPA's recommended action level for indoor radon is 4 pCi/L to protect against lung cancer. Radon concentrations in excess of 20 pCi/L have been measured in buildings in the area, and abatement measures have been taken at many locations. Since some of the uranium concentrations in groundwater exceed safe drinking water standards and some homes in the area have excessive indoor radon, it is important to understand the source of the uranium in the groundwater and the processes involved. Low-grade uranium deposits are found in several areas of the Española Basin in the Tesuque Formation and actually form the San Jose mining district (Fig. 1; McLemore and Chenoweth, 1989). Low-grade uranium deposits also are found in the Proterozoic rocks in the San Jose and Nambe mining districts in the Sangre de Cristo Mountains adjacent to the Española Basin. Numerous rhyolitic volcanic ash beds, some in various stages of alteration, and sandstones with volcanic detritus are found interbedded within the Tesuque Formation that also could contribute uranium to the basin.

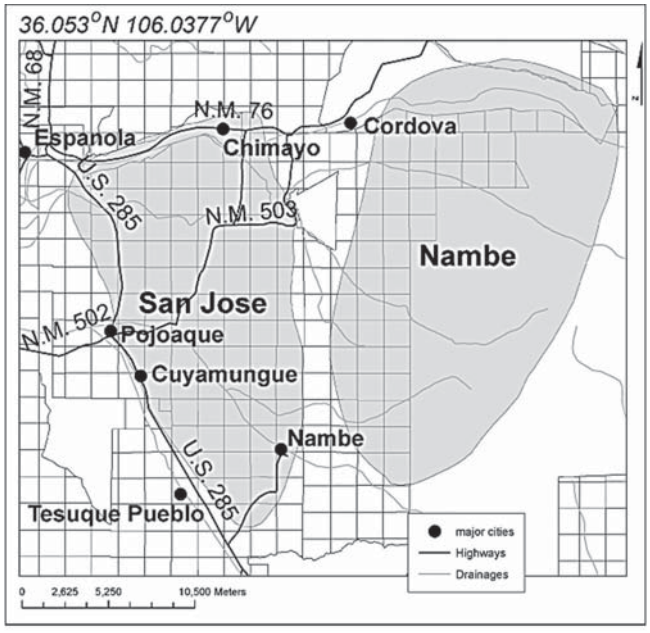

FIGURE 1. Location of San Jose and Nambe mining districts (shaded), Santa Fe County, New Mexico (T19-21N, R8, 9E). Latitude and longitude (in NAD27) refers to upper left corner of the figure. The Santa Fe Buckman well field is southwest of this area.

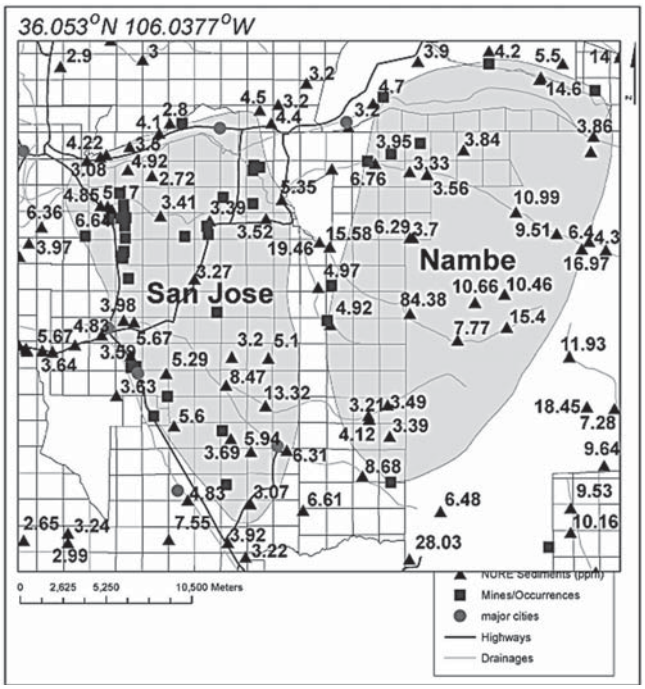

FIGURE 2. Location of NURE stream sediment samples in the San Jose and Nambe mining districts. Stream-sediment samples containing greater than 12 ppm U are considered anomalously high (McLemore, 2010a, b). Note that high uranium concentrations are found in drainages in the Nambe district (up to 84 ppm), which are related to radioactive pegmatites, veins, and replacements that are in Proterozoic granitic and metamorphic rocks.

The purposes of this paper are to 1) summarize the geology, geochemistry, and uranium occurrences within the mining districts in and adjacent to the Española Basin, 2) present a model for the formation of the uranium occurrences in the rocks and waters in the basin, and 3) comment briefly on the future economic potential and environmental concerns of uranium deposits in the San Jose and Nambe mining districts. Detailed geology and stratigraphy of the districts are described in cited references and are only summarized here.

This ongoing investigation of mineral resources in New Mexico includes updates and revisions of prior work by McLemore (1983), McLemore et al. (1984), Chenoweth (1979), and McLemore and Chenoweth (1989). Published and unpublished data were inventoried and compiled on existing mines within the San Jose and Nambe districts. Mineralized areas were examined and sampled in 2011. Geochemical data were obtained from published sources and collected samples.

MINING AND EXPLORATION HISTORY

Uranium minerals were found in the Tesuque Formation in the Española Basin in July 1954 by L.E. Rogers, Q.B. Rogers, and H.R. Rogers (Chenoweth, 1979). Soon after, geologists with the U.S. Atomic Energy Corporation conducted an aerial radiometric survey in the Española Basin area and found additional uranium occurrences in the Tesuque Formation and in Proterozoic rocks (Fig. 4; Tables 1 and 2; Collins and Freeland, 1956; Hilpert, 1969; U.S. Atomic Energy Commission, 1970; Chenoweth, 1979). One small mine, the San Jose No. 13 (NMSF0033), produced 12 lbs (5 kg) of U_3O_8 at a grade of 0.05% U_3O_8 in 1957 (Table 2). Since this ore was below the grade set by the U.S. Government of 0.10% U_3O_8, the ore was considered to be no-pay ore, and no further shipments were sent. In the late 1970s and early 1980s, exploration companies examined the Española Basin and drilled in several locations, but the results were not encouraging and exploration for uranium was discontinued.

GEOLOGIC SETTING

The Española Basin joins the San Luis Basin to the north and the Santo Domingo Basin to the south and is bounded by the Proterozoic-cored Sangre de Cristo Mountains on the east and the Picuris Mountains to the north, and the Jemez Mountains and Pajarito Plateau on the west. The Española Basin is filled with Oligocene-Miocene sedimentary rocks (older Tesuque Formation and younger Chamita Formation of the Santa Fe Group) and with Pliocene to Holocene sedimentary rocks (Ancha Formation, terrace deposits, modern sediments) and lava, tuff, and volcaniclastic sedimentary rocks from the Jemez Mountains volcanic field.

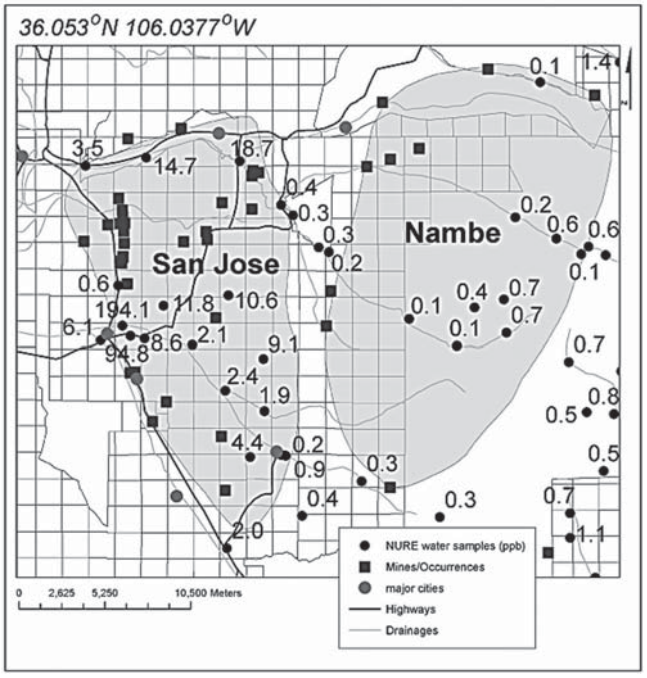

FIGURE 3. Location of NURE water samples in the San Jose and Nambe mining districts. Water samples containing greater than 6 ppb U are considered anomalously high (McLemore, 2010a, b). The EPA safe drinking water standard is 30 ppb. Note that waters near Pojoaque contain up to 194 ppb uranium, but waters in the south closer to Santa Fe are less than 4 ppb.

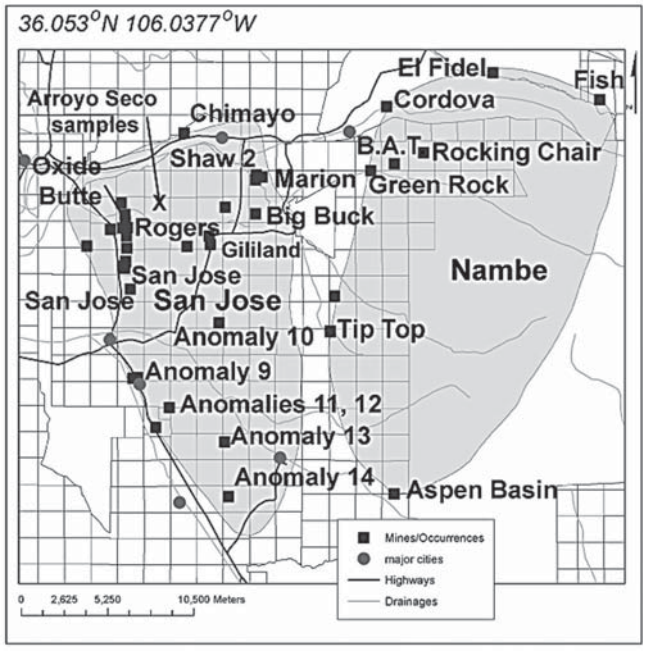

FIGURE 4. Location of mines and prospects in the San Jose and Nambe mining districts. Location of San Jose mine is latitude 35.938417°, longitude 106.013496° (NAD27).

The Tesuque Formation consists of several hundred to 2500 meters of silty sandstone and sandstone with minor conglomerate, siltstone, and mudstone that was deposited in the late Oligocene and Miocene (Koning, 2002; Koning et al., 2002, 2004, 2007a, b; Johnson et al., 2008; Koning and Read, 2010). Several rhyolitic volcanic ash beds and sandstones with volcanic detritus are interbedded with the sedimentary rocks in the Tesuque Formation. Sediments of the Tesuque Formation in the eastern Española Basin in the area of interest were derived from the Proterozoic rocks in the Sangre de Cristo Mountains to the east and the Peñasco embayment to the north (Koning and Read, 2010). The Española Basin is unusual for Rio Grande rift basins, in that there are many rhyolitic volcanic ash beds exposed at and near the surface interbedded with the Tesuque Formation that can provide uranium to the groundwater.

DESCRIPTION OF URANIUM DEPOSITS

Nambe mining district

The Nambe mining district is in the western Sangre de Cristo Mountains in Santa Fe and Rio Arriba Counties, where several northeast-trending pegmatites intruded the Proterozoic rocks (Table 1) that consist of quartz, microcline, perthite, plagioclase, muscovite, tourmaline, garnet, magnetite-ilmenite, beryl, and other minerals, including uranium and thorium minerals. Pegmatites are coarse-grained granitic dikes, lenses, pods, or veins and represent the last and most hydrous phase of crystallizing magmas. Nearly all of the pegmatites in New Mexico and adjacent areas are Proterozoic in age and intruded metamorphic and granitic rocks. Most pegmatites in New Mexico and adjacent areas are associated with the Late Proterozoic granitic plutonism at 1450-1400 Ma (see McLemore, 2011). The pegmatites vary in size, but are typically several hundred meters long and up to several tens of meters wide. Simple pegmatites consist of feldspar, quartz, and mica, whereas complex pegmatites are mineralogically and texturally zoned and consist of a variety of rare minerals. Uranium and thorium are found in many pegmatites as discrete uranium and thorium minerals, or as impurities in other pegmatite minerals (Redmond, 1961; Hilpert, 1969; Chenoweth, 1979; McLemore, 1983). Several commodities have been produced from complex pegmatites elsewhere in New Mexico in the past, including mica, beryl, Li, U, Th, REE, feldspar, Nb, Ta, W, and gem stones, but production form the Nambe district is small, yielding small amounts of beryl and mica (Table 1). Additional commodities occur in pegmatites that could be recovered, including quartz, Sb, Rb, and Mo (Jahns, 1946; McLemore et al., 1988a, b). Typically minerals containing these rare commodities are scattered discontinuously throughout the pegmatite, thereby hampering economic recovery.

TABLE 1. Mines and occurrences in the Nambe mining district, Santa Fe and Rio Arriba Counties.

Mine Id Number	Mine Name	Location (section, township, range)	Latitude (decimal degrees)	Longitude (decimal degrees)	Commodities (bold=produced)
NMRA0154	**El Fidel**	22,23 T21N, R11E	36.039535	-105.7626198	**Be**, mica
NMRA0155	**Fish**	29, T21N, R12E	36.024663	-105.6900059	**Be**
NMSF0067	unknown	34, T20N, R10E	35.9166362	-105.8702569	Mica
NMSF0086	Aspen Basin	1, 12, T118N, R10E	35.8077856	-105.8299956	Ta, Mica, Au, Ag, Bi, Be
NMSF0087	B.A.T.	1, T20N, R10E	35.9895638	-105.8293787	mica, Be
NMSF0088	Big Buck	18, T20N, R10E	35.9620643	-105.9235874	Be
NMSF0089	**Green Rock**	2, T20N, R10E	35.98555	-105.84555	**Mica**
NMSF0090	**Rocking Chair**	6, 31, 36, T20, 21N, R10, 11E	35.99555	-105.80972	**Mica, Be,** Ta
NMSF0091	**Tip Top**	1, T20N, R10E	35.8972	-105.87322	**Mica,** Be
NMSF0092	unknown	5, T19N, R10E			Mica

Notes: Data from Redmond, 1961; McLemore et al., 2002; unpublished NMBGMR file data). All are pegmatite deposits.* Bold names were producing mines.

TABLE 2. Mines and occurrences in the San Jose mining district, Santa Fe County.

Mine Id Number	Mine Name	Location (section, township, range)	Latitude (decimal degrees)	Longitude (decimal degrees)	Commodities (bold=produced)
NMSF0025	Marion	7, T20N, R10E	35.982278	-105.918917	Cu, U, mica
NMSF0034	Shaw 2	7, T20N, R10E	35.983417	-105.922917	Cu, U, mica, Be
NMSF0149	unknown	7, T29N, R10E	35.980676	-105.923553	U, mica
NMSF0001	Anomaly 1	32, T20N, R9E	35.920583	-106.008444	U, V
NMSF0003	Anomaly 2, 3	33, T20N, R9E	35.949611	-105.954889	U, V
NMSF0005	Anomaly 4	24, 25, T20N, R9E	35.944111	-106.037944	U, V
NMSF0006	Anomaly 5	13, T20N, R9E	35.965639	-105.943944	U, V
NMSF0007	Anomalies 6, 7	22, T20N, R9E	35.943972	-105.970111	U, V
NMSF0008	Anomaly 8	17, T19N, R9E	35.872035	-106.003263	U, V
NMSF0009	Anomaly 9	17, T19N, R9E	35.871629	-106.006676	U, V
NMSF0010	Anomaly 10	2, T19N, R9E	35.901833	-105.948167	U, V
NMSF0011	Anomalies 11, 12	22, 28, T19N, R9E	35.855508	-105.981966	U, V
NMSF0012	Anomaly 13	36, T19N, R9E	35.83648	-105.944503	U, V
NMSF0013	Anomaly 14	12, T18N, R9E	35.806362	-105.94201	U, V
NMSF0019	Gilliland Claims	23, T20N, R9E	35.945056	-105.954083	U, V
NMSF0023	J C Roybal	19, T20N, R9E	35.953389	-106.021833	U, V
NMSF0028	Rogers	17, T20N, R9E	35.967979	-106.014586	U, V
NMSF0029	Rogers	17, 29, T20N, R9E	35.957806	-106.011583	U, V
NMSF0030	Rogers	20, T20N, R9E	35.954333	-106.010222	U, V
NMSF0031	Rogers	20, T20N, R9E	35.94975	-106.010861	U, V
NMSF0032	Rogers	20, T20N, R9E	35.942972	-106.010556	U, V
NMSF0033	**San Jose***	29, T20N, R9E	35.932059	-106.012266	**U, V**
NMSF0150	San Jose	29, T20N, R9E	35.932208	-106.012845	U, V
NMSF0151	San Jose	29, T20N, R9E	35.932765	-106.013007	U, V
NMSF0152	San Jose	29, T20N, R9E	35.933164	-106.012768	U, V
NMSF0153	San Jose	29, T20N, R9E	35.935185	-106.011597	U, V
NMSF0154	San Jose	29, T20N, R9E	35.935735	-106.011493	
NMSF0155	San Jose	29, T20N, R9E			U, V
NMSF0156	unknown	29, T19N, R9E	35.844527	-105.991343	U, V
NMSF0157	unknown	20, T20N, R9E	35.954074	-106.013523	U, V
NMSF0158	Oxide Butte	17, T20N, R9E	35.961536	-106.011777	U, V

Notes: Data from from Redmond, 1961; Collins and Freeland, 1956; Hilpert, 1969; U.S. Atomic Energy Commission, 1970; Chenoweth, 1979; McLemore et al., 2002; unpublished NMBGMR file data).
All mines and occurrences are sandstone uranium deposits except for NMSF0025, which is a pegmatite, and NMSF0034 and NMSF0149, which are vein and replacement deposits in Proterozoic rocks (McLemore and Chenoweth, 1989).
* Bold indicates a producing mine.

San Jose mining district

Uranium deposits are found in the San Jose mining district in the Española Basin (Fig. 4, Table 2) as: 1) sandstone uranium deposits in the Tesuque Formation, 2) veins and replacements in Proterozoic rocks (formerly Precambrian vein and replacement deposits after McLemore, 2001), and 3) Proterozoic pegmatites (McLemore and Chenoweth, 1989; McLemore et al., 2002). Three types of sandstone uranium deposits are found in the San Jose district: 1) medium-grained sandstone with uranium associated with clay galls and carbonaceous material, 2) poorly consolidated fine- to medium-grained sandstone with disseminated uranium and little carbonaceous material, and 3) coarse-grained sandstone to conglomerate with abundant uranium associated with carbonaceous material. Carnotite ($K_2(UO_2)_2V_2O_8 \cdot 3H_2O$), schroekingerite ($NaCa_3(UO_2)(CO_3)SO_4)F \cdot 10H_2O$), and meta-autunite ($Na_2(UO_2)_2(PO_4)_2 \cdot 6\text{-}8H_2O$) coat fractures and bedding surfaces in sandstone, siltstone and mudstone within the Tesuque Formation, especially near clay galls and carbonaceous material (Chenoweth, 1979). Uranium in the San Jose district also occurs as coatings around opal and chert grains, with organic debris, in clay zones, and in fossil bone fragments within the Tesuque Formation.

A small fault block of Proterozoic rocks lies within the northeast corner of the San Jose mining district, where three uranium occurrences are found (Table 2). At the Shaw 2 prospect (New Mexico Mines Database Number NMSF0034) in section 7, T20N, R10E (35.9827424°N 105.9221679°W), pits and two short adits expose vein and replacement deposits consisting of secondary uranium minerals disseminated along a shear zone (N20°E), approximately 1 m thick, in Proterozoic amphibo-

lite schist intruded by simple quartz-feldspar-biotite pegmatites and granite. The uranium minerals are reported to be associated with secondary copper minerals. Hematite, quartz, biotite, feldspar, and unknown uranium minerals are found along fractures within the shear zone. Radioactivity is approximately 50 times above background (background 30 cps, high 1,500 cps). Reid et al. (1982) reported a sample contained 47 ppm U. Chemical analyses of samples collected for this report are in Table 3. Some pegmatites in this area also contain localized high concentrations of uranium.

MINERALOGY AND LEACHING ANALYSES OF TESUQUE FORMATION URANIFEROUS SEDIMENTS

Four samples of uraniferous sediments from the Tesuque Formation were selected for mineralogical analysis by X-ray diffraction (XRD), deionized (DI) water leaching to extract water-soluble constituents, and EPA 3050 Method acid leaching to extract species not soluble in water but considered "environmentally available." The XRD data were collected on splits of the same samples used for leaching studies; XRD analyses were performed on a Siemens D500 diffractometer using finely ground powders. Results of XRD analysis are summarized in Table 4. Solution compositions of leachates were determined by inductively coupled plasma-mass spectrometry (ICP-MS) (using a PE-SCIEX ELAN 6100), inductively coupled plasma-optical emission spectroscopy (ICP-OES) (using a Perkin-Elmer Optima 2100DV), and ion chromatography (IC) (Dionex-Summit). The DI water leachates were prepared from 100 g samples treated with 150 g DI water. The EPA Method 3050 leachates were prepared using 2 to 2.5 g samples treated with HNO_3, HCL, and H_2O_2 (for analysis by ICP-OES) or HNO_3 and H_2O_2 alone (for analysis by ICP-MS). Results of leachate analysis are summarized in Appendix 1.

Field relationships and images of the samples analyzed are shown in Fig. 5a for sandstone samples from Arroyo Seco and in Fig. 5b for clay samples from Oxide butte. The two sandstone samples from bank exposures along Arroyo Seco (N 35.96804°, W 106.00674°, Fig. 5) are clay-poor sands with yellow/orange discoloration and strong response from a scintillometer. The two clay samples from Oxide butte (N 35.96162°, W 106.01234°, NMSF0158, Table 2, Fig. 5) are associated with sands of strong yellow/orange discoloration and are respectively from a clay-rich basal channel deposit (Oxide butte basal clay A) and from a clay ball higher within the channel deposit (Oxide butte clay ball D).

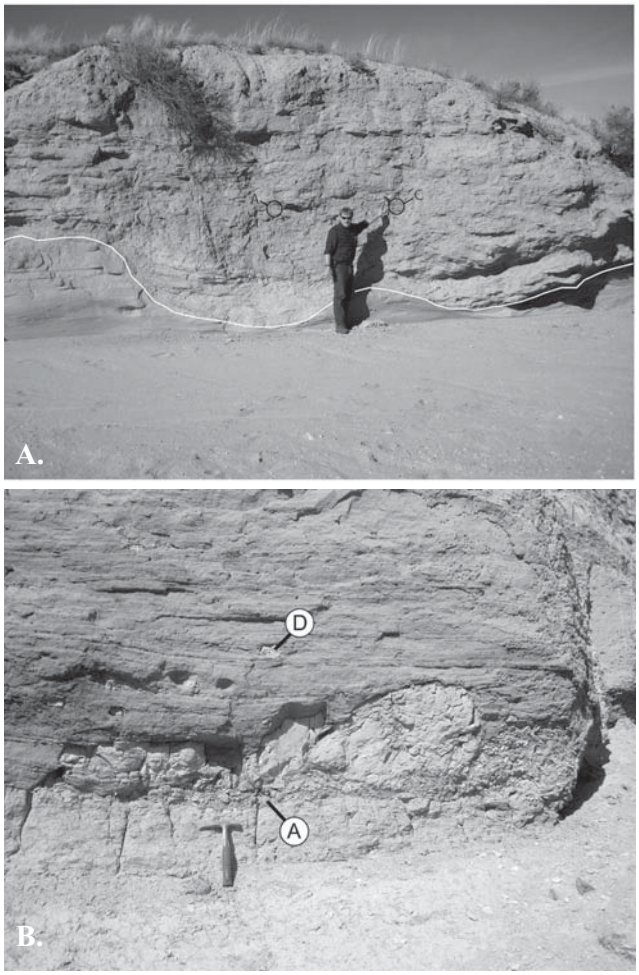

FIGURE 5. A. Locations of sandstone samples A and C collected at Arroyo Seco. The white line at the bottom of the image marks the base of a channel scoured into Tesuque Formation fine sandstone and filled by coarser uraniferous sandstone. B. Locations of basal clay gall A and clay ball D samples collected at Oxide butte.

TABLE 3. Chemical analyses of Proterozoic and Tesuque Formation samples analyzed by a portable X-ray Fluorescence instrument (Bruker model Tracer III).

Sample	Description	Mn ppm	La ppm	Ce ppm	Cr ppm	Ni ppm	Cu ppm	Zn ppm	Th ppm	U ppm	Y ppm
Shaw1	Shaw 2 (NMSF0034)	2412	124	226	203	115	60	99	6	48	45
Shaw2	Shaw 2 (NMSF0034)	1745			163	45	65	81			36
SJ1	San Jose mine (NMSF0033)	374			22					25	26
SJ1a	San Jose mine (NMSF0033)	319		65	50		11	22	29	255	45
SJ2	San Jose mine (NMSF0033)	286			25			7	5	83	21
bone	Found in Tesuque sandstone	237			5		12	64	91	371	146

These clay-rich samples had weaker scintillometer signals but were still above background.

Table 4 summarizes the major differences in mineralogy between the uraniferous sandstones (Arroyo Seco samples) and clays associated with a uraniferous sandstone (Oxide butte samples). The discolored uraniferous sandstones from Arroyo Seco are friable and poorly cemented, lacking either smectite or calcite cement. The sandstones from Arroyo Seco contain a significant amount of microcline in addition to plagioclase, reflecting a major sand component derived from Proterozoic granitic rocks. The clay-rich samples from Oxide butte have little or no microcline and contain calcite (analysis of the associated yellow/orange sands at Oxide butte, not shown here, is similar to the sands at Arroyo Seco in lacking calcite and having only trace amounts of smectite).

Preliminary data from an oriented and glycolated clay separate of clay ball D at Oxide butte show a very poorly developed 001 peak that separates on glycolation into an 18.0 Å smectite, an illitic clay or severely altered mica, and a 10.5 Å phase tentatively identified as palygorskite. In contrast, the small amount of clay (~2%) that could be extracted from the sand at Oxide butte is a relatively simple smectite that expands to 17.1 Å on glycolation. The varieties of clay minerals at Oxide butte that occur in ball form and as galls, along with altered micas and dispersed smectites in the discolored sandstone, suggest a complex range of clay minerals, some of which could act as hosts for uranium accumulation.

The leachate data in Appendix 1 reveal high concentrations of water-soluble anions in the Arroyo Seco sandstone matrix, including bromide (0.03-0.08 mg/g), chloride (9-23 mg/g), nitrate (0.2-0.8 mg/g), oxalate (0-0.3 mg/g), phosphate (0.6-5 mg/g), and sulfate (2-12 mg/g). In contrast, these anions are below detection in the clays from Oxide butte. At Arroyo Seco, the uranium soluble in water is 26% to 48% of the total extractable uranium as determined in ICP-MS analysis of the Method 3050 acid leachates; comparable water soluble to total extractable ratios are observed for the clay samples at Oxide butte (37% to 48%). The relative mobility of uranium in both the sandstone and the clays may be similar but the low permeability of the clays versus the higher permeability of the sandstones may account for the higher concentrations of uranium in sandstone (66-108 µg/g vs. 8-14 µg/g). Further evidence of mobility and accumulation of uranium in the sandstone can be found in the much higher U/Th ratios within the sandstone (11-22) compared with the clays (U/Th < 2).

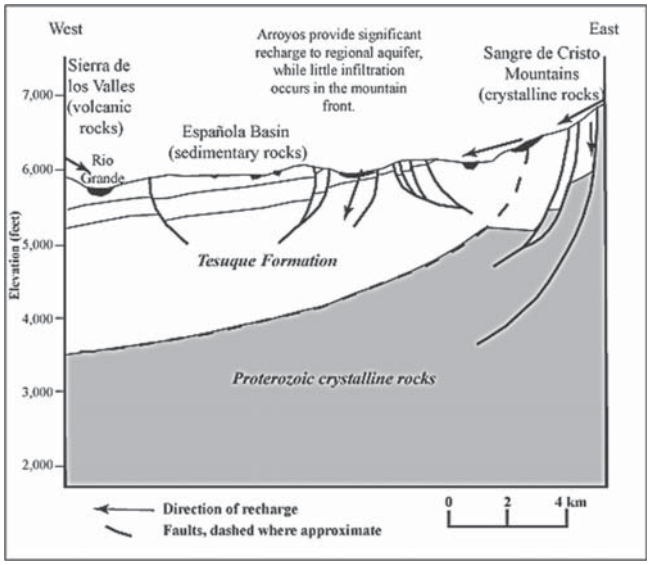

FIGURE 6. Schematic cross section through the Española Basin showing flow of modern groundwater. Uranium is precipitated in sandstones of the Tesuque Formation. Figure modified from J. Shomaker and Associates (unpubl. consultant report for ASCG INC. re. Aamodt feasibility study, 2003).

SOURCE OF URANIUM

The sandstone uranium occurrences in the Tesuque Formation probably represent natural precipitation and concentration from uraniferous groundwaters, likely derived from 1) volcanic ash beds within the Tesuque Formation, 2) the alteration of granitic and volcanic detritus within the sedimentary host rocks, and 3) Proterozoic rocks in the Sangre de Cristo Mountains to the east (Fig. 6). Uranium in modern groundwaters likely was derived from the same sources, as well as from leaching and oxidation of older uranium occurrences in the Tesuque Formation (Table 2). Green clay lenses in the Tesuque Formation could have formed from the alteration of volcanic ash beds. Typical granites contain 5-10 ppm U and pegmatites locally can contain as much as several percent U. Uranium-bearing minerals are found in many pegmatite deposits in the Sangre de Cristo Mountains (McLemore, 1983). Volcanic ash beds and volcanic detritus are well known sources of uranium in sandstones and the leaching studies further support this source (Zielinski, 1978; Walton et al., 1981; Kizis

TABLE 4. Quantitative XRD analyses (wt%) of samples splits representing those leached by deionized water and EPA 3050 acid methods (see Appendix Table A1 for leachate data; Fig. 5a, b for location of samples).

sample	illite-smectite	mica	amphibole	quartz	plagioclase	microcline	calcite
Arroyo Seco A	-	tr	tr	53	35	12	-
Arroyo Seco C	~1-2	tr	-	54	28	16	-
Oxide Butte A (NMSF0158)	68	tr	-	19	4	-	9
Oxide Butte D (NMSF0158)	45	tr	-	34	15	-	6

tr = trace amount (<1%); dash = not detected

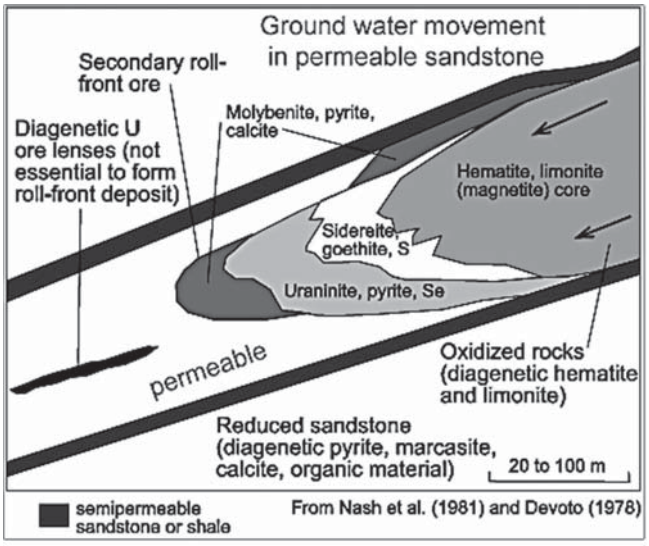

FIGURE 7. Sketch of the formation of roll-front sandstone uranium deposits. Oxidizing groundwaters migrated through the uranium deposits and remobilized some of the primary sandstone uranium deposits. Uranium was reprecipitated ahead of the oxidizing waters forming roll-front sandstone uranium deposits.

and Runnels, 1984; George-Aniel et al., 1991; Subramanyam et al., 1997). Although no leaching studies of granitic rocks are available, Stuckless and Nkomo (1978) discuss granitic rocks as a possible source of sandstone uranium deposits.

DEPOSITION MODEL OF URANIUM IN THE ESPAÑOLA BASIN

Geochemical studies suggest that modern groundwater flow in the Española Basin is complex (Fig. 6; Johnson et al., 2008). Water flowing down dip from the Sangre de Cristo Mountains likely contains uranium derived from the Proterozoic granite and low-grade uranium deposits in both the Española Basin and the area surrounding Santa Fe. Uranium also is leached from Tesuque Formation volcanic ash beds and sandstones with volcanic detritus. These uranium-bearing volcanic ash beds are mostly found in the Española Basin and typically are not as common elsewhere in the Rio Grande rift. Uranium precipitated from the groundwaters to form the roll-front sandstone uranium deposits at the interface of oxidizing (i.e., meteoric waters) and reducing conditions (Fig. 7). Uranium precipitated at reduced zones formed by clay, organic material, and possibly at the interface of reduced basin waters. Erosion and lowering of the water table in the sediments within the Española Basin likely began between 3.0 and 7 Ma, when the Rio Grande formed an integrated drainage system (Dethier et al., 1988; Smith, 2004). The uranium roll-front deposits were emplaced in the sandstones of the Tesuque Formation before this erosion and shortly after deposition of the early-middle Miocene sediments of the Tesuque Formation.

Continued oxidation and leaching of uranium from the uranium sources and from older uranium deposits in the Tesuque Formation and Proterozoic rocks then formed the modern geochemical anomalies that affect today's groundwater (Fig. 8). Erosion from Proterozoic rocks formed the geochemical anomalies found in the stream sediments. Radon results from the decay of uranium-bearing minerals in the rocks and groundwater.

FUTURE ECONOMIC POTENTIAL AND ENVIRONMENTAL CONCERNS

The uranium occurrences in the San Jose and Nambe mining districts are too discontinuous, too small, and too low grade to be considered for economic development at the present time. The Española Basin does provide a modern analog to the formation of roll-front uranium deposits and additional research on the mineralogy and chemical composition of the source rocks is recommended.

These occurrences likely have been leached in modern time and have contributed to high uranium concentrations in the groundwater and to high radon concentrations, along with leaching of rhyolitic volcanic ash deposits, sandstones with volcanic detritus, and Proterozoic rocks. The uranium in groundwater is natural and not contamination caused by man (i.e. not anthropogenic). Homes with high indoor radon levels can be remediated (http://www.epa.gov/radon/, accessed on 3/24/11). Water wells with high concentrations of uranium also can be remediated. Some area residents have installed anion exchange and reverse osmosis treatment units to decrease uranium in their water supply. Anion exchange units installed on two wells serving a mobile home park exhibited a decrease in uranium from ~100 µg/L to less than 5 µg/L. The units use proprietary resins to exchange uranyl carbonates with chloride, and are regenerated with potassium chloride brine. Disposal of waste generated by drinking-water treatment systems is an emerging issue.

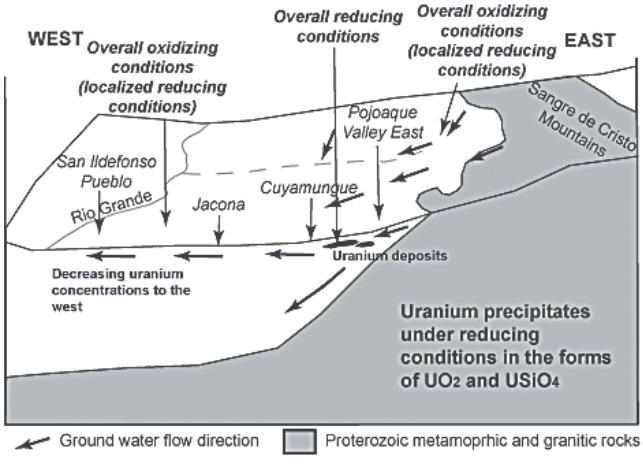

FIGURE 8. Schematic model of the formation of uranium deposits.

CONCLUSIONS

Detail geologic and hydrologic studies of the Española Basin over the last decade have provided a better understanding of the geology and hydrology of the basin and can be incorporated into a geologic model for the formation of uranium deposits found in the Tesuque Formation, which also provides an explanation for the high concentrations of uranium found in water supply wells and radon in homes in the area. Shortly after the Tesuque Formation was deposited, water began leaching uranium from the volcanic ash beds and volcanic detritus within the sediments. Uranium also was being leached out of the Proterozoic rocks where uranium is found in pegmatites, veins and replacement deposits (Tables 1, 2), and within granitic rocks. The uraniferous-waters migrated through sandstones and uranium was precipitated in the vicinity of clay beds, organic material, bones, and perhaps at the interface with reducing groundwaters to form the sandstone uranium deposits typical of roll-front uranium deposits (Fig. 7). As the groundwater level within the Tesuque Formation lowered, the Tesuque Formation was exposed to weathering and additional leaching of uranium from the volcanic ash beds, volcanic detritus, and older sandstone uranium deposits continued to occur and increased the levels of uranium in the groundwater today (Fig. 8). These processes are still active. Radon is likely derived from the high concentrations of uranium in the groundwater, and not from the small sandstone uranium deposits, which are above the current groundwater table.

The uranium deposits found in the Española Basin are small, discontinuous, and low grade and will not constitute an economic resource in the near future. The high levels of uranium within water supply wells and the high levels of indoor radon found in homes in the area are natural, derived from leaching of uranium from the rocks, and not caused by human activities. Several methods of remediation are available to lower the uranium in water supplies (anion exchange and reverse osmosis treatment units that remove uranium) and to reduce indoor radon levels (http://www.epa.gov/radon/, accessed on 3/24/11).

ACKNOWLEDGMENTS

This paper is part of an on-going study of the mineral resources of New Mexico at NMBGMR (Peter Scholle, Director and State Geologist) and of the distribution and source of uranium in groundwater in the Española Basin by the New Mexico Environment Department and Los Alamos National Laboratory (LANL). Work at LANL was supported through cooperation with the New Mexico Small Business Assistance Program. This manuscript was reviewed by Bill Carey and Shari Kelley and their comments were helpful and appreciated.

REFERENCES

Chenoweth, W.L., 1979, Uranium in the Santa Fe area, New Mexico: New Mexico Geological Society, 30th Field Conference Guidebook, p. 261-264.

Collins, G.E., and Freeland, R.E., 1956, A report in the airborne radiometric survey and ground geologic reconnaissance in the Española area New Mexico: U.S. Atomic Energy Commission, Report RME-1075, 16 p.

Dethier, D.P., Harrington, C.D., and Aldrich, M.J., 1988, Late Cenozoic rates of erosion in the western Española basin, New Mexico: Evidence from geologic dating of erosion surfaces: Geological Society of America Bulletin, v. 100, p. 928-937.

Devoto, R.H., 1978, Uranium in Phanerozoic sandstone and volcanic rock, *in* Short course in uranium deposits; their mineralogy and origin: American Geological Institute, Short Course Handbook 3, p. 293-305.

George-Aniel, B., Leroy, J.L., and Poty, B., 1991, Volcanogenic uranium mineralization in the Sierra Pena Blanca district, Chihuahua, Mexico: Three genetic models: Economic Geology, v. 86, p. 233-248.

Hakonson-Hayes, A.C., Fresquez, P.R., and Whicker, F.W., 2002, Assessing potential risks from exposure to natural uranium in well water: Journal of Environmental Radioactivity, v. 99, p. 29-40.

Hilpert, L.S., 1969, Uranium resources of northwestern New Mexico: U.S. Geological Survey, Professional Paper 603, 166 p.

Jahns, R.H., 1946, Mica deposits of the Petaca district, Rio Arriba County, New Mexico, with a brief description of the Ojo Caliente district, Rio Arriba County and the Elk Mountain district, San Miguel County: New Mexico Bureau of Mines and Mineral Resources, Bulletin 25, 294 p.

Johnson, P.S., Koning, D.J., Timmons, S.W., and Felix, B., 2008, Geochemical characterization of groundwater in the southern Española Basin, Santa Fe, New Mexico: New Mexico Bureau of Geology and Mineral Resources, Open-file Report 511, 55 p.

Kizis, J.A., Jr., and Runnels, D.D., 1984, The mobility of uranium and associated trace elements in the Bates Mountain Tuff, central Nevada: Economic Geology, v. 79, p. 558-564.

Koning, D.J., 2002, Preliminary geologic map of the Española 7.5-minute quadrangle, Rio Arriba and Santa Fe Counties, New Mexico: New Mexico Bureau of Geology and Mineral Resources, Geologic Open-file Report OF-GM 54, scale 1:24,000.

Koning, D.J. and Read, A.S., 2010, Geologic map of the southern Espanola Basin, Santa Fe County, New Mexico, New Mexico Bureau Geology Mineral Resources, Open-file Report OF-531, scale 1:45000.

Koning, D.J., Nyman, M., Horning, R., Eppes, M., and Rogers, S., 2002, Preliminary geologic map of the Cuidiyo quadrangle, Santa Fe County, New Mexico: New Mexico Bureau of Geology and Mineral Resources, Open-file Digital Geologic Map OF-GM 56, 39 p.

Koning, D.J., Smith, G., Lyman, J., and Paul, P., 2004, Lithosome S of the Tesuque Formation: hydrostratigraphic and tectonic implications of a newly delineated lithosome in the southern Española Basin, New Mexico, *in* Hudson, M.R., ed., Geologic and hydrogeologic framework of the Española basin – Proceedings of the 3rd annual Española basin workshop, Santa Fe, New Mexico: U.S. Geological Survey Open-file Report 2004-1093, p. 17.

Koning, D.J., Smith, G.A., and Read, A., 2007a, Cenozoic stratigraphy in the Santa Fe embayment and northwards to the Buckman well field, Española basin, NM, *in,* Borchert, C.I., ed., Geologic and hydrogeologic framework of the Española basin – Proceedings of the 6th Annual Española Basin workshop, Santa Fe, New Mexico, March 6, 2007: New Mexico Bureau of Geology and Mineral Resources, Open-file Report 508, p. 2.

Koning, D.J., Broxton, D., Sawyer, D., Vaniman, D., and Shomaker, J., 2007b, Surface and subsurface stratigraphy of the Santa Fe Group near White Rock and the Buckman areas of the Española Basin, north-central New Mexico: New Mexico Geological Society, 58th Fall Field Conference Guidebook, p. 209-224.

McLemore, V.T., 1983, Uranium and thorium occurrences in New Mexico: distribution, geology, production, and resources; with selected bibliography: New Mexico Bureau of Mines and Mineral Resources, Open-file Report OF-182, 950 p., also U.S. Department of Energy Report GJBX-11(83).

McLemore, V. T., 2001, Silver and gold occurrences in New Mexico: New Mexico Bureau of Mines and Mineral Resources, Resource Map 21, 60 p.

McLemore, V.T., 2010a, Use of the New Mexico Mines database and ArcMap in uranium reclamation studies: Society of Mining, Metallurgy and Exploration Annual Convention, Phoenix, Feb 2010, Preprint 10-125

McLemore, V.T., 2010b, Use of the New Mexico Mines database and ArcMap in uranium reclamation studies: Society of Mining, Metallurgy and Exploration Transactions, in press.

McLemore, V.T., 2011, Geology and mineral resources in the Hopewell and Bromide No. 2 districts, northern Tusas Mountains, Rio Arriba County, New Mexico: N.M. Geological Society, 62nd Field Conference Guidebook, p. 379-388.

McLemore, V. T. and Chenoweth, W. L., 1989, Uranium resources in New Mexico: New Mexico Bureau of Mines and Minerals Resources, Resource Map 18, 36 p.

McLemore, V.T., Roybal, G.H., Broadhead, R.F., Chamberlin, R., North, R.N., Osburn, J.C., Arkell, B.W., Colpitts, R.M., Bowie, M.R., Anderson, K., Barker, J.M. and Campbell, F., 1984, Preliminary report on the geology and mineral resource potential of the northern Rio Puerco resource area in Sandoval and Bernalillo counties and adjacent parts of McKinley, Cibola and Santa Fe counties, New Mexico: Open File Report 211, 348 p.

McLemore, V.T., North, R.M., and Leppert, S., 1988a, Rare-earth elements (REE), niobium and thorium districts and occurrences in New Mexico: New Mexico Bureau of Mines and Mineral Resources, Open-file Report OF-324, 28 p.

McLemore, V.T., North, R.M., and Leppert, S., 1988b, Rare-earth elements (REE) in New Mexico: New Mexico Geology, v. 10, p. 33-38.

McLemore, V. T., Donahue, K., Krueger, C. B., Rowe, A., Ulbricht, L., Jackson, M. J., Breese, M. R., Jones, G., and Wilks, M., 2002, Database of the uranium mines, prospects, occurrences, and mills in New Mexico: New Mexico Bureau of Geology and Mineral Resources, Open file Report 461, CD-ROM.

McQuillan, D., Longmire, P., Johnson, P., Kulis, J., Martinez, F., Counce, D., and Keating, E., 2005, Natural uranium in groundwater in the Española Basin, *in* McKinney, D.C., ed., Geologic and hydrologic framework of the Española Basin—Proceedings of the 4th annual Española Basin workshop, Santa Fe, New Mexico, March 1-3, 2005: U.S. Geological Survey, Open-file Report 2005-1130, p. 11.

Nash, J.T., Granger, H.C. and Adams, S.S., 1981, Geology and concepts of genesis of important types of uranium deposits, *in* Skinner, B.J., ed., 75th Anniversary Volume: Economic Geology, 1905-1980, p. 63-116.

Redmon, D.E., 1961, Reconnaissance of selected pegmatite districts in north-central New Mexico: U.S. Bureau of Mines, Circular 8013, 79 p.

Reid, B.E., Griswold, G.B., Jacobsen, L.C., and Lessard, R.H., 1982, Santa Fe quadrangle, New Mexico: U.S. Department of Energy, Report PGJ/F-021(82), 41 p.

Smith, G.A., 2004, Middle to late Cenozoic development of the Rio Grande rift and adjacent regions in northern New Mexico, *in* Mack, G.H., and Giles, K.A., eds., The Geology of New Mexico, A Geologic History: New Mexico Geological Society, Special Publication 11, p. 331-358.

Stuckless, J.S. and Nkomo, I.T., 1978, Uranium-lead isotope systematics in uraniferous alkali-rich granites from the Granite Mountains, Wyoming: Implications for uranium source rocks: Economic Geology, v. 73, p. 427-441.

Subramanyam, A.V., Gupta, K.R., Basu, A.N., and Balakrishnan, S.P., 1997, Volcanic tuff in the lower Mahadek Formation of Meghalaya Plateau: Implications on uranium source: Journal of Atomic Mineral Science, v. 5, p. 73-79.

U.S. Atomic Energy Commission, 1970, Preliminary reconnaissance for uranium in New Mexico, 1950-1958: U.S. Atomic Energy Commission, Report REM-160, p. 156.

Walton, A.W., Galloway, W.E. and Henry, C.D., 1981, Release of uranium from the volcanic glass in sedimentary sequences: An analysis of two systems: Economic Geology, v. 76, p. 69-88.

Zielinski, R.A., 1978, Uranium abundances and distribution in associated glassy and crystalline rhyolites of the western United States: Geological Society of America, Bulletin, v. 89, p. 409-414.

APPENDIX 1. Leachate solution analyses for samples from Arroyo Seco and Oxide butte

Arroyo Seco		H_2O content %	Ag µg/g	Al µg/g	As µg/g	B µg/g	Ba µg/g	Be µg/g	Br µg/g	Ca µg/g	Cd µg/g	Cl µg/g	Li µg/g
DI leachates													
	Sandstone A	1.90	<0.079	<0.158	2.05	0.642	0.846	<0.08	29.3	4260	<0.079	9316	11.84
	Sandstone C	2.51	<0.060	<0.119	2.22	0.108	0.515	<0.06	75.3	5445	<0.060	22750	16.88
3050 leachates													
ICPOES	Sandstone A			5239		6.3	720			29093			26
ICPOES	Sandstone C			10447		11.6	182			5092			58
ICPMS	Sandstone A		<22	4221	133		482	<22			<22		19
ICPMS	Sandstone C		<25	8089	19.8		158	<25			<25		40

Oxide Butte		H_2O content %	Ag µg/g	Al µg/g	As µg/g	B µg/g	Ba µg/g	Be µg/g	Br µg/g	Ca µg/g	Cd µg/g	Cl µg/g	Li µg/g
DI leachates													
	Basal clay A	5.83	<0.026	<0.052	2.96	<0.052	0.73	<0.03	0	1645	<0.026	0	3.83
	Clay ball D	4.28	<0.035	0.202	5.08	<0.070	2.67	<0.04	0	3165	<0.035	0	6.73
3050 leachates													
ICPOES	Basal clay A			29681		14.7	133			89730			76
ICPOES	Clay ball D			19069		19.9	187			33778			91
ICPMS	Basal clay A		<23	21601	14.08		149	<23			<23		77.6
ICPMS	Clay ball D		<22	19191	81.44		190	<22			<22		87

Arroyo Seco		Mg µg/g	Mn µg/g	Mo µg/g	Na µg/g	Ni µg/g	NO_2 µg/g	NO_3 µg/g	Oxalate µg/g	Pb µg/g	PO_4 µg/g	Rb µg/g	Sb µg/g
DI leachates													
	Sandstone A	539	<0.079	50.88	17308	0.751	<0.79	776	<0.79	<0.016	4.743	0.390	0.739
	Sandstone C	770	0.071	48.37	26243	0.739	<0.60	232	295	<0.012	0.597	0.433	0.130
3050 leachates													
ICPOES	Sandstone A	3844	140.4		447								
ICPOES	Sandstone C	7609	432.9		1271								
ICPMS	Sandstone A		96.2	6.35		<22				<4		<22	<0.9
ICPMS	Sandstone C		240.7	3.60		<25				9.5		<25	<1.0

APPENDIX 1 (CONT.)

Oxide Butte		Mg µg/g	Mn µg/g	Mo µg/g	Na µg/g	Ni µg/g	NO_2 µg/g	NO_3 µg/g	Oxalate µg/g	Pb µg/g	PO_4 µg/g	Rb µg/g	Sb µg/g
DI leachates													
	Basal clay A	186	<0.026	0.441	1491	<0.026	0	0	0	<0.005	0	0.406	0.065
	Clay ball D	333	<0.035	0.943	1775	0.252	0	0	0	<0.007	0	0.464	0.055
3050 leachates													
ICPOES	Basal clay A	14209	464.5		859								
ICPOES	Clay ball D	12206	351.6		307								
ICPMS	Basal clay A		448.7	<0.9		27.16				13.8		33.48	<0.9
ICPMS	Clay ball D		404.0	<0.9		26.68				11.4		32.27	<0.9

Arroyo Seco		Se µg/g	Si µg/g	SO_4 µg/g	Sn µg/g	Sr µg/g	Th µg/g	Ti µg/g	Tl µg/g	U µg/g	V µg/g	Zn µg/g
DI leachates												
	Sandstone A	40.9	847	1950	<0.079	57	<0.079	<0.158	0.099	52.21	0.67	0.22
	Sandstone C	222.1	719	12286	<0.060	76	<0.060	<0.119	0.273	17.22	1.36	0.18
3050 leachates												
ICPOES	Sandstone A		147			110		331				34.53
ICPOES	Sandstone C		85			88		384				49.00
ICPMS	Sandstone A	<22			<0.9	70	5		<22	107.80	<22	26.74
ICPMS	Sandstone C	<25			<1.0	77	6		<25	65.85	<25	39.03

Oxide Butte		Se µg/g	Si µg/g	SO_4 µg/g	Sn µg/g	Sr µg/g	Th µg/g	Ti µg/g	Tl µg/g	U µg/g	V µg/g	Zn µg/g
DI leachates												
	Basal clay A	95.8	408	<0.026	0	20	<0.026	<0.052	<0.026	3.21	0.03	0.17
	Clay ball D	185.2	551	<0.035	0	39	<0.035	<0.070	<0.035	6.59	0.09	0.31
3050 leachates												
ICPOES	Basal clay A		195			448		204				68.91
ICPOES	Clay ball D		187			201		77				58.39
ICPMS	Basal clay A	68.1			<0.9	239	11		<23	8.48	<23	61.68
ICPMS	Clay ball D	29.9			<0.9	214	8		<22	13.87	30.03	59.63